Journal of Ceramic Processing Research. Vol. 19, No. 2, pp. 179~182 (2018)

J O U R N A L O F
Ceramic Processing Research

Effects of high-energy ball milling of commercial Y_2O_3 powders on their densification using spark plasma sintering

Cheol Woo Park, Jung Hun Lee, Suk Hyun Kang, Jae Hwa Park, Hyun Mi Kim, Hyo Sang Kang, Hee Ae Lee, Joo Hyung Lee, Jun Hyeong In, and Kwang Bo Shim*

Division of Advanced Materials Science and Engineering, Hanyang University, Seoul 04763, Korea

Commercial Y_2O_3 powders were treated by high-energy ball milling (HEBM) and then subjected to spark plasma sintering (SPS) in a furnace at 1600 °C under 30 MPa for 5 minutes to produce pure Y_2O_3 transparent ceramics. The sintered Y_2O_3 bodies show a relative density of about 99.52% and a grain size of about 3.2 μm, which is approximately six times smaller than that of the specimen obtained using commercial powders. This result shows that HEBM is highly effective in improving the sinterability of Y_2O_3 with the controlled grain growth. The transmittance of all sintered specimen was similar in the infrared region (2000 nm), but the specimen that underwent HEBM showed excellent transmittance in the visible light region (700 nm). In particular, the hardness and fracture strengths of the sintered bodies that underwent HEBM were 8.48 GPa and 0.91 MPa·$m^{1/2}$, respectively, demonstrating excellent mechanical characteristics.

Key words: Y_2O_3 transparent ceramics, Spark plasma sintering, High energy ball milling, Densification.

Introduction

Y_2O_3 has been extensively researched as a promising material for optical applications owing to its high melting point (2430 °C), high corrosion resistance, thermal stability, and broad transparency (0.2-8 μm) [1-6]. Furthermore, it has a cubic crystal (Ia3) structure with optical isotropy, and is therefore ideal for manufacturing transparent ceramics [7]. Y_2O_3 transparent ceramics are known as the best IR window material since they have a higher and broader range of transmittance than most other materials (sapphire, AlON, YAG, $MgAl_2O_4$) [6, 8]. IR window materials must provide mechanical protection for sensors, and permeability for transmission and reception, under extreme-use environments, as they are used as heat seeking sensor window [9-10]. Therefore, IR window materials require high strength; however, Y_2O_3 transparent ceramics are weaker in heat resistance and fracture strength, compared to the abovementioned transparent ceramics [11], and methods to improve these are being researched on. C.B. Willingham argued that a sintered body achieves close to its maximum strength when the grain size is in the range of 1-10 μm, and also reported that the fracture strength of ceramics doubled or tripled for Y_2O_3 transparent ceramics that were produced using nano powders [8]. In other words, the initial powder grain size should be reduced in order to suppress the final grain size of the sintered bodies.

Recently, the high-energy ball milling (HEBM) method, which allows for extreme comminutions, has been regarded as an efficient process to improve the mechanical properties of sintered ceramics, by producing nano powders with a uniform grain size [12, 13]. In general, powders with a small grain size have higher sinterability due to their large specific surface area [14-16], and it is more advantageous to produce completely dense ceramics because it is easier to remove pores in the grain boundary diffusion sintering process [17, 18].

Spark plasma sintering (SPS) can provide a dense sintering and controlled grain growth; the sintering process occurs in a very short time, and at a low temperature, compared to many other sintering methods (e.g., pressureless sintering, hot press, hot isostatic pressing, etc.) [19-20].

In this study, transparent Y_2O_3 ceramics were produced by spark plasma sintering (SPS) and limiting the grain size of the sintered bodies after processing commercial Y_2O_3 powders by HEBM. The effect of HEBM was evaluated by analysing the characteristics of the produced Y_2O_3 sintered bodies.

Experiment

Powder preparation and SPS densification

As the source material, commercially available highly pure Y_2O_3 powders (99.99% pure, 220 nm, Cenotec, Korea) were milled at 700 rpm together with 1 mm diameter zirconia balls at the weight ratio of 10:1

*Corresponding author:
Tel : +82-2-2220-0501
Fax: +82-2-2291-7395
E-mail: kbshim@hanyang.ac.kr

for 7 hrs using the HEBM (PM-400, Retsch, Germany). The milled Y_2O_3 powders had an average diameter of approximately 85 nm, and were dried in an electric oven at 60 °C for 24 hrs. The powders were then inserted into a graphite die with an inner diameter of 15 mm surrounded by a graphite foil, and sintered using an SPS system (Sumitomo Coal Mining, S-515S, Japan) in 10 Pa vacuum, and a uniaxial pressurized condition of 30 MPa. The temperature was elevated from room temperature to 1600 °C at a rate of 100 °C/min and then maintained for 5 min for achieving the sintering condition. Upon completion of sintering, the pressure was released and the current was blocked. The sintered specimen was annealed in an oxygen atmosphere in an electric furnace to 1000 °C for 4 hrs at an elevation rate of 10 °C/min. Both sides of the specimen were polished for the evaluation of optical properties.

Characterization

The morphologies of the powders before and after HEBM and the average grain size of each fabricated specimen were analysed at an acceleration voltage of 5 -15 kV using a field emission scanning electron microscope (FE-SEM, NOVA Nano SEM 450, FEI, Czech Republic). The specimen for analysis with a transmission electron microscope (TEM, Jeol, JEM-2100F, Japan, analysis at 200 kV) was prepared using a focused ion beam (FIB, FEI, Scios, Czech Republic). The relative density was measured using the Archimedes method, and the in-line transmittance was determined using a UV-Vis-NIR spectrophotometer (Lambda 950, Perkin-Elmer, America) in the wavelength range of 250 -2000 nm. The average Vickers hardness and fracture toughness were determined by 15 indentations using a digital hardness tester (FV-700e, FUTURE-TECH Co. Ltd, Japan).

Results and Discussion

The FE-SEM images of commercial Y_2O_3 powders and HEBM Y_2O_3 powders are shown in Fig. 1. The initial Y_2O_3 particles were of irregular sizes and shapes, and in aggregate forms, with an average size of 220 nm. After HEBM, the average grain size of Y_2O_3 decreased to 85 nm, and the powders had an uniform distribution of grain sizes and showed individual spheres with no aggregates.

Fig. 2 shows the images of the final fabricated specimens, and the resulting transmittance spectra after SPS of commercial Y_2O_3 powders and Y_2O_3 powders that have undergone HEBM (hereinafter, the sintered bodies are referred to as COMM-SPSed and HEBM-SPSed, respectively). Both specimens clearly show the letters at the back, but the letters appearing by using the HEBM-SPSed specimen are slightly brighter than those by the COMM-SPSed specimen. An analysis of

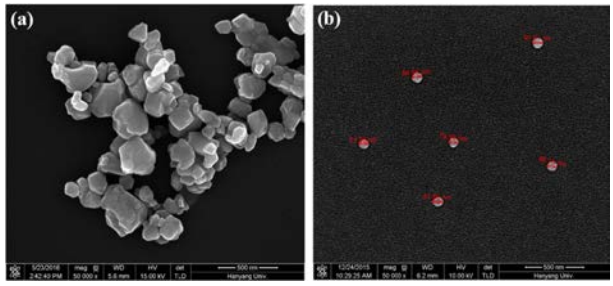

Fig. 1. FE-SEM images of the Y_2O_3 powders (a) before HEBM (b) after HEBM.

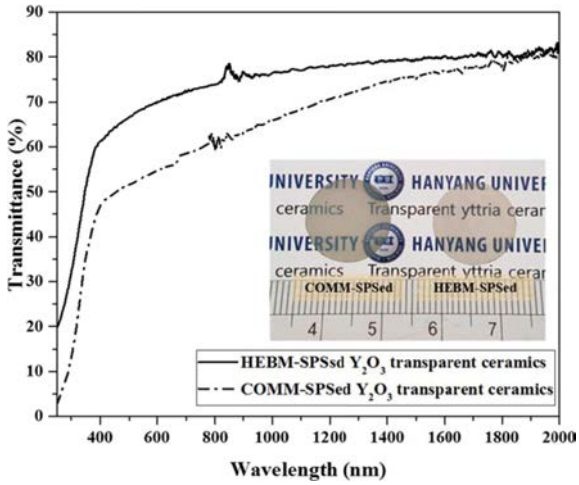

Fig. 2. Transmittance spectra of the COMM-SPSed and HEBM-SPSed Y_2O_3 transparent ceramics.

the transmittance spectra revealed that the COMM-SPSed and HEBM-SPSed specimens have high transmittances of 81.15% and 82.41%, respectively in the near-infrared region (2000 nm). However, the transmittance of the COMM-SPSed Y_2O_3 transparent ceramics was 58.50% at $\lambda = 700$ nm, and 65.78% at $\lambda = 1000$ nm. The HEBM-SPSed specimen showed a transmittance of 72.29% at $\lambda = 700$ nm and 76.43% at $\lambda = 1000$ nm. These results indicate that the HEBM-SPSed specimen has better transmittance in the visible light region than the COMM-SPSed specimen. This is because the micropores in the COMM-SPSed specimen are larger or greater in number than those in the HEBM-SPSed specimen, and when the light passes through the ceramics in the nanometre range, a higher scattering is activated [22].

Fig. 3 shows the etched surface of the specimens that are processed by SPS. The microstructure of the HEBM-SPSed specimen was much finer than that of the COMM-SPSed specimen sintered under the same conditions. The COMM-SPSed specimen (Fig. 3(a)) had much larger and smaller pores than those of the HEBM-SPSed specimen (Fig. 3(b)) (indicated by white arrows). In the COMM-SPSed specimen with pores, the transmittance decreased after light scattering and absorption. On the other hand, the HEBM-SPSed

specimen (b) showed a dense microstructure and densely sintered bodies, and the micropores were difficult to observe in the FE-SEM image. Furthermore, the absence of abnormally grown grains suggests that densification occurred in a thermodynamically stable condition.

The low transmittance of the COMM-SPSed specimen implies that the micro pores as well as pores smaller than micro pores may be the cause of light scattering [19]. Fig. 4 shows the TEM image indicating the sizes and shapes of the pores in (a) SPSed specimen, and (b) HEBM-SPSed specimen. The occluded nanopores remaining at the triple junction of the SPSed specimen are indicated by white arrows (Fig. 4(a)); occluded nanopores of approximately 65 nm and 9.38 nm sizes can be observed on the right. In contrast, the HEBM-SPSed specimen shows very clean grain boundaries with no occluded pores, as illustrated in Fig. 4(b). The low porosity and dense microstructure resulted in a high transmittance.

Fig. 5 shows the average grain sizes and the relative density data of the COMM-SPSed and HEBM-SPSed specimens. K. Serivalsatit has reported that the grain boundary of ceramics plays the function of dislocation blocking, and a smaller grain size of ceramics indicates a higher hardness [7]. Thus, the grain size is an

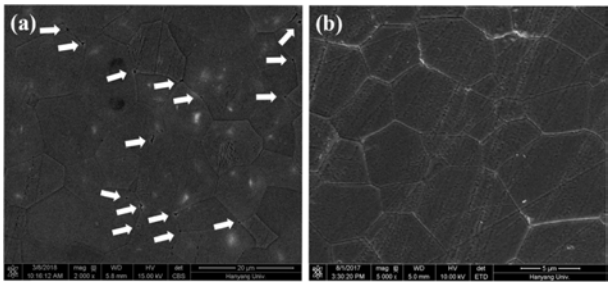

Fig. 3. FE-SEM image of the etched surface of (a) COMM-SPSed and (b) HEBM-SPSed Y_2O_3 ceramics.

important factor that determines the mechanical characteristics of ceramics. In particular, it has been reported that ceramics with a grain size of 1-10 μm have very high fracture strength and thermal shock resistance [8]. As shown in the figure, the average grain size of the (a) HEBM-SPSed specimen (3.2 μm) is approximately six times smaller than that of the (b) COMM-SPSed specimen (18.6 μm). The relative density thus increased from 98.96% to 99.52% by employing HEBM. Therefore, it seems that because the powders were already controlled to the nano-size and had high surface energy through HEBM, they progressed to the closest packing in a short time by SPS [12, 13].

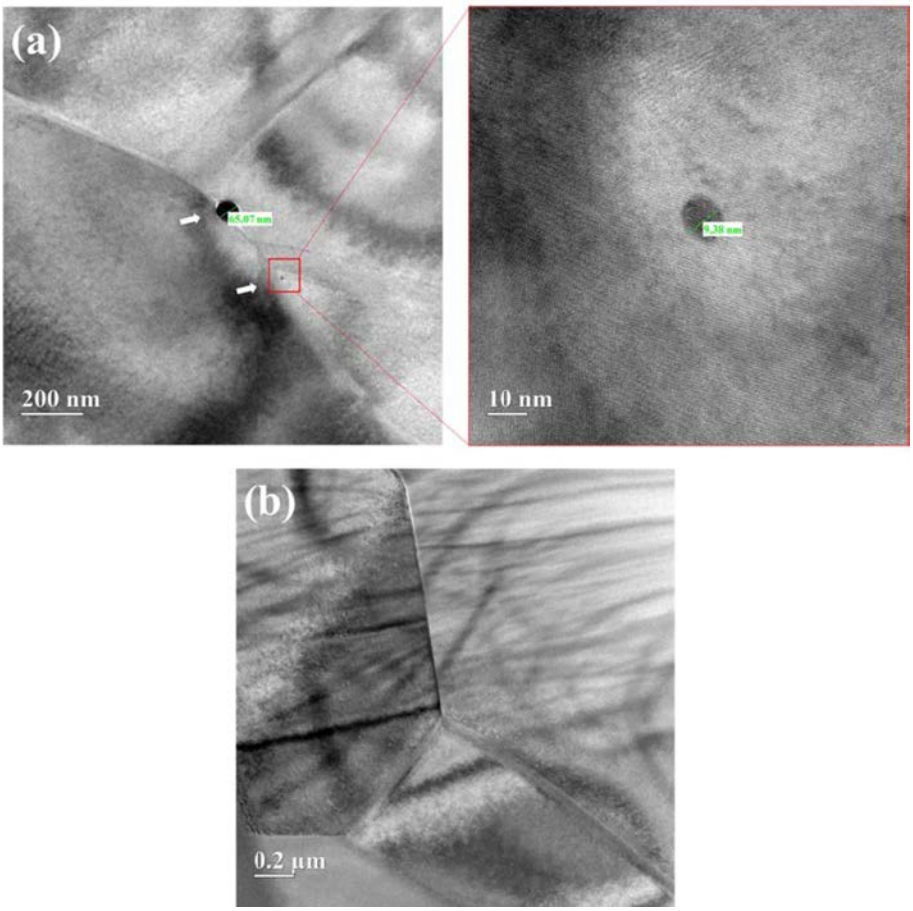

Fig. 4. TEM images of (a) COMM-SPSed and (b) HEBM-SPSed Y_2O_3 sample showing the presence of occluded nanopores, and straight grain boundary at the triple junction.

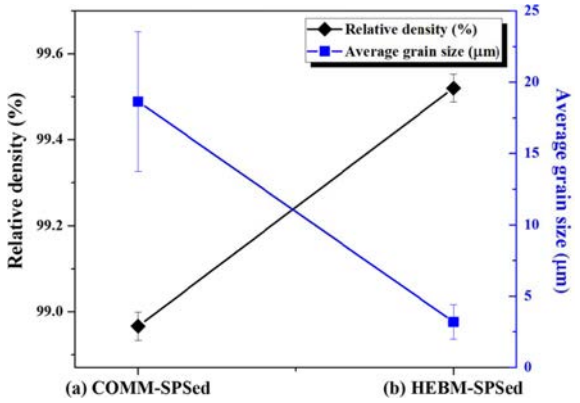

Fig. 5. Variation of relative density and average grain size of the COMM-SPSed and HEBM-SPSed Y_2O_3 specimens.

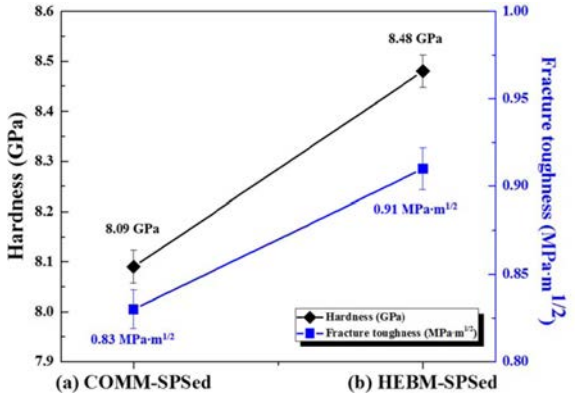

Fig. 6. Vickers hardness and fracture toughness of the COMM-SPSed and HEBM-SPSed Y_2O_3 transparent specimens

Fig. 6 shows the Vickers hardness and fracture toughness data of the COMM-SPSed and HEBM-SPSed specimens. The (a) COMM-SPSed and (b) HEBM-SPSed specimens showed hardness values of 8.09 GPa and 8.48 GPa, respectively. In the case of fracture toughness, as with the Vickers hardness, the HEBM-SPSed specimen (0.91 MPa·$m^{1/2}$) shows a better value than that of the COMM-SPSed specimen (0.83 MPa·$m^{1/2}$). These results confirm that low porosity, high relative density, and small grain size are critical factors for improving mechanical characteristics.

Conclusions

In this study, pure Y_2O_3 transparent ceramics were successfully manufactured by the SPS within 5 minutes at 1600 °C under 30 MPa using commercial Y_2O_3 powders, and nano-sized powders produced by HEBM. The residues of micro- and nano-sized pores were controlled well in the HEBM-SPSed specimen compared to the COMM-SPSed specimen. The increased surface energy of the Y_2O_3 powders after HEBM was very effective in achieving full densification of 99.52% within a very short period. The HEBM-SPSed specimen showed a transmittance similar to that of the COMM-SPSed specimen in the infrared region (2000 nm), which improved to 72.29% in the visible light region (700 nm). Because the grain size of the sintered body was controlled, the mechanical characteristics improved; the hardness increased from 8.09 to 8.48 GPa and fracture strength from 0.83 to 0.91 MPa·$m^{1/2}$.

References

1. J.R. Lu, K. Takaichi, T. Uematsu, A. Shirakawa, M. Musha, K. Ueda, Jpn. J. Appl. Phys. Part 2-Letters 41 (2002) L1373.
2. M. Ivanov, Y. Kopylov, V. Kravchenko, L. Jiang, A. Medvedev, PAN Yubai, J. Rare Earths. 32 (2014) 254.
3. W.J. Tropf, M.E. Thomas, R.K. Frazer, SPIE 5078 (2003) 80-89.
4. S.F. Wang, J. Zhang, D.W. Luo, et al., Prog. Solid State Chem. 41 (2013) 20-54.
5. P. Hogan, T. Stefanil, C. Willingham, R. Gentilman, 10th DoD Electromagnetic Windows Symposium (2004).
6. L. An, A. Ito, T. Goto, J. Eur. Ceram. Soc. 32 (2012) 1035-1040
7. K. Serivalsatit, B. Kokuoz, B. Yazgan-Kokuoz, M. Kennedy, J. Ballatow, J. Am. Ceram. Soc. 93 (2010) 1320.
8. C.B. Willingham et al., SPIE Proc. 5078 (2003) 179.
9. H. Zhang, B.N. Kim, K. Morita, H. Yoshida, K. Hirag, and Y. Sakka, J. Am. Ceram. Soc. 94 (2006) 3206-3210.
10. Y. Sun, S. Shimai, X. Peng, G. Zhou, H. Kamiya, S. Wang, Ceram. Int. 40 (2014) 8841-8845.
11. H.R. Khosroshahi, H. Ikeda, K. Yamada, N. Saito, K. Kaneko, K. Hayashi, and K. Nakashima, J. Am. Ceram. Soc. 95 (2012) 3263-3269.
12. L.B. Kong, W. Zhu, O.K. Tan, Mater. Lett. 42 (2000) 232-239.
13. L.B. Kong, J. Ma, W. Zhu, O.K. Tan, Mater. Lett. 51 (2001) 108-114.
14. S. Zhang, J. Liu, J. Feng, C. Li, X. Ma, P. Zhang, J. Materiomics. 1 (2015) 118-123.
15. X. Zhang, Z. Zhang, B. Nie, H. Chen, Y. Wang, L. Zheng, Y. Bai, W. Wang, Ceram. Int. 44 (2018) 10766-10772.
16. L. Feng, S.H. Lee, H.N. Kim, J. Eur. Ceram. Soc. 37 (2017) 1891-1898.
17. Y. Hirata, I. A. Aksay, and R. Kikuchi, J. Ceram. Soc. Jpn. 98 (1990) 126-35
18. K.H. Sim, G. Wang, T.J. Kim, K.S. Ju, J. Alloy. Compd. 741 (2018) 1112-1120.
19. K.H. Kim, J.H. Chae, J.S. Park, J.P. Ahna and K.B. Shim, J. Ceram. Proc. Res. 10 (2009) 716-720.
20. K.H. Kim and K.B. Shim, Mater. Charact. 50 (2003) 31-37.
21. S.H. Shim, J.W. Yoon, K.B. Shim, J. Matsushita, B. S. Hyun and S. G. Kang, J. Alloy. Compd. 413 (2006) 188-192.
22. K. Ning, J. Wang, D. Luo, J. Ma, J. Zhang, Z.L. Dong, L.B. Kong, D.Y. Tang, Opt. Mater. 50 (2015) 21-24.